

LOCAL-SCALE CLIMATE VARIABILITY AND TRENDS IN A VULNERABLE RURAL LANDSCAPE, NORTHWEST ETHIOPIA

Aimro Likinaw^{1*}, Arragaw Alemayehu² and Woldeamlak Bewket¹

^{1*} Corresponding author

Department of Geography & Environmental Studies
Addis Ababa University

² Department of Geography & Environmental Studies
Debre Berhan University

Email: aimro.likinaw@aau.edu.et

ABSTRACT

This study analyses local-scale climate variability and trends in northwest Ethiopia, covering three food-insecure and vulnerable districts, namely Lay Gaynt, Tach Gaynt, and Simada. We examined temperature and rainfall data on 4×4 km grids. The coefficient of variation and standardized anomaly index were used to assess the variability of rainfall and temperature. As a result, annual and seasonal rainfall show high inter-annual variability, except for the major rainy season (*Kiremt*), which shows a moderate coefficient of variation. The proportion of negative anomalies ranges from 39% (Lay Gayint) to 65% (Simada) over the observation period. Moreover, trend analysis was conducted using the Mann-Kendall (MK) and Innovative Trend Analysis (ITA) tests. The MK test for annual rainfall exhibited a significant rising trend for the Lay Gayint and Tach Gayint districts. The ITA for annual and seasonal rainfall indicated positive trends for Lay Gayint and Tach Gayint, while negative trends were observed in Simada. The ITA and MK tests showed similar increasing tendencies in seasonal and annual temperatures. The MK technique revealed positive patterns in 28 time series and negative patterns in 20 time series for monthly, seasonal, and annual rainfall data, whereas the ITA method revealed positive trends in 23 time series and negative trends in 25 time series. The results of this study are useful for local development planning that should take into account current and possible future climate patterns.

Key Words: *MK, ITA, Trend, Rainfall, and Temperature, Ethiopia.*

INTRODUCTION

Climate change is one of the most pressing global concerns of the twenty-first century (Abidoye & Odusola, 2015). Developing countries are particularly susceptible as their principal economic activities rely on climate-sensitive products with limited adaptability (Mesfin et al., 2020). Weather and climate extremes affect the majority of Sub-Saharan African countries, including Ethiopia, causing low agricultural production (Amare & Simane, 2017). Ethiopia's climate has evolved in recent decades, with temperatures rising by 0.4°C in the last four decades (Gebrechorkos et al., 2019). Since the 1990s, Ethiopia has experienced a decrease in rainfall

(Abebe, 2017), which has significantly influenced the country's agricultural production and water availability.

The El Niño Southern Oscillation (ENSO) and an increase in anthropogenic activities both significantly contributed to the reported variations in climate across the country (Diro et al., 2012; Rowell et al., 2015). According to recent literature (Dubache et al., 2019; Minda et al., 2018), the rainfall patterns over East Africa are largely determined by inter-oceanic processes and large-scale atmospheric phenomena. High-pressure systems in the Indian and Atlantic oceans are primarily responsible for the variability in rainfall over East Africa. Due to the variations in altitude and terrain, determining historical climatic patterns and future estimates for Ethiopia can be a difficult task (Philip et al., 2018). The country's rainfall patterns are quite diverse, with some places seeing only one rainy season while others have two or more (Ayalew et al., 2012). Recent studies on multidecadal climate variability in East Africa, particularly Ethiopia, have yielded contradictory results. Various studies have found decreasing annual rainfall in various sections of Ethiopia, whereas others have found rising rainfall patterns. For instance, Alemayehu and Bewket (2017) found rising trends in annual and *Kiremt* rainfall but a significantly declining trend in *Belg* rainfall. *Kiremt* is the main rainy season for most parts of Ethiopia, covering the period from June to September, while *Belg* is the short rainy period for most parts of Ethiopia from March to May. Asfaw et al. (2018) reported significant declining trends in *Kiremt* and annual rainfall, but a subtle decline in *Belg* rainfall. In the northern highlands of Ethiopia, Miheretu (2020) observed an increasing trend in *Kiremt* rainfall, but *Belg* rainfall exhibited a declining trend. Moreover, Gebrehiwot et al. (2019) suggested decreasing trends in *Kiremt* and *Belg* season rainfall. Therefore, it is critical to conduct trend and variability analyses of rainfall and temperature patterns to accurately predict climate extremes and take appropriate adaptation and mitigation actions.

Methodologically, previous studies used parametric techniques such as the t-test and linear regression in trend identification studies (Benti & Abara, 2019; Hundera et al., 2019). These techniques, however, have limitations because they require a normally distributed data. Other researchers applied non-parametric techniques like the Mann-Kendal (MK) test without considering serial association in the data set (Ayalew et al., 2012; Chala et al., 2020; Miheretu, 2020). For these reasons, several studies have suggested the application of a modified MK test, which is efficient in the presence of auto-correlation (Hamed & Rao 1998). Moreover, Sen (2012) suggested the Innovative Trend Analysis (ITA) test, which does not necessitate assumptions like non-normality, collinearity, or length of time series data. Therefore, the present study applies the ITA technique to local climate data analysis, which has not been conducted before in the study districts and compares the results of the ITA with those of the modified MK test. This study is useful for context-specific planning of climate risk management and local development in the study area, where agriculture depends on rainwater and constitutes almost the sole means of subsistence for the population.

METHODOLOGY

The Study Site

The study site includes three districts (*woredas* in *Amharic*), namely Lay Gayint, Tach Gayint, and Simada in the South Gondar Zone Administration (Figure 1). Lay Gayint is in the *High Dega* (3200–3700 m asl) agro-ecological zone, and Tach Gayint and Simada are in the *Dega* (2300–3200 m asl) and *Woyana Dega* (1500–2300 m asl) agro-ecological zones, respectively (Hurni et al., 2016). The area is a heavily degraded part of the country because of a long history

of settlement and cultivation, overgrazing, and other socioeconomic and policy-related factors (Getachew, 2017). Extensive farming and shrubland dominate the current land cover. The main rainy season (*Kiremt*) occurs from June to mid-September, and the short rainy season (*Belg*) occurs from March to May (Rosell, 2011). The short rainy season is inconsistent with crop failures, making *Belg* harvesting difficult (Rosell, 2011). The study area currently lacks food due to late-onset, early termination, and poor *Belg* performance. Furthermore, steep topography and barren mountains accelerate runoff, resulting in land degradation and, as a result, low production. Hence, the area is part of the country's drought-stricken and food-insecure areas. The farming system is a mixed crop-livestock, characterized by intensive and continuous cropping. Barley (*Hordium vulgare*), wheat (*Triticum aestivum*), maize (*Zea mays*) and tef (*Eragrostis tef*) are the main cereals grown in the area. Cattle, sheep, goats, and equines are the dominant livestock raised. The benefit of livestock to people's livelihoods is limited due to the frequency of livestock diseases (Getachew, 2017). Crop production is affected by erratic rainfall, poor soil fertility, small per capita landholding, poor per acre land and limited use of improved agricultural technologies (Ayalew et al., 2012). Low agricultural productivity is further affected by its dependence on unreliable rainfall. The overall result is that a majority of households do not harvest sufficient food and depend largely on food assistance or are supported by the Productive Safety Nets Program (PSNP). According to information obtained from the South Gondar Zone Administration office, five districts benefited from the PSNP, including the study area (Libokemkem, Ebnat, Simada, Lay Gayint, and Tach Gayint). Non-farm livelihood activities are not well established due to inadequate access to infrastructure, ineffective and inefficient agricultural marketing system, and limited access to institutional support services, to name a few.

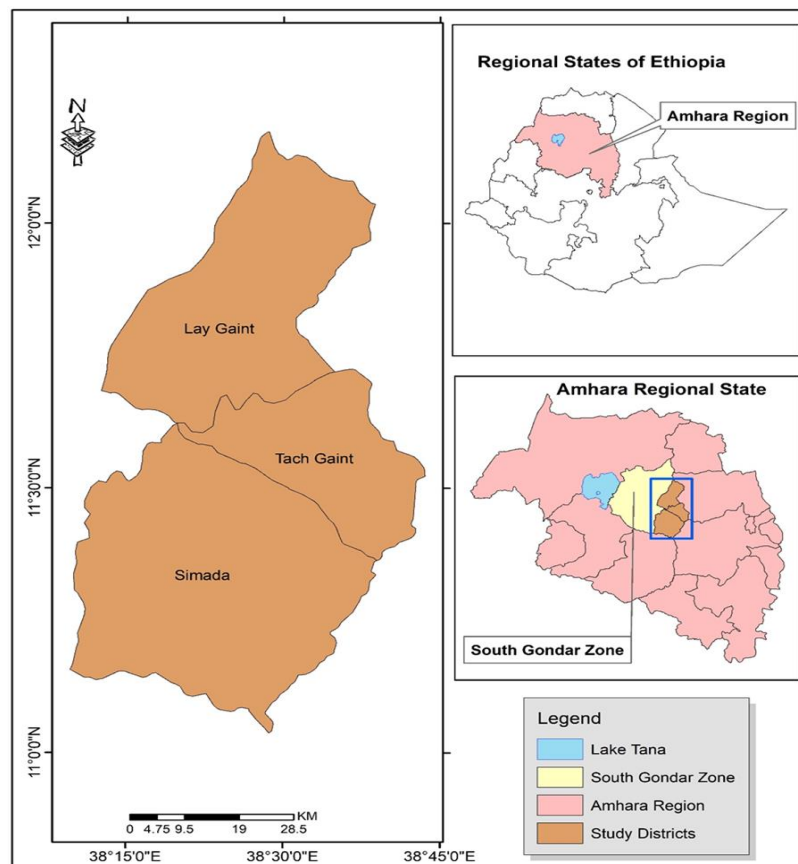


Figure 1. Study site location

MATERIALS AND METHODS

Data type and source

The study used temperature and rainfall data extracted from the Enhancing National Climate Services (ENACTS) dataset obtained from the National Meteorological Agency (NMA) of Ethiopia. ENACTS is a 4×4 km gridded dataset reconstructed from meteorological satellites and weather stations covering the period from 1981 to 2018. ENACTS has been calibrated and validated, revealing robust performance when weighed at station sites in Ethiopia (Dinku et al., 2018). Because ENACTS data were chosen for analysis, (1) there are many missing values in station datasets (Asfaw et al., 2018), and (2) most stations are new and do not have enough data records to perform trend analysis (Alemayehu & Bewket, 2017; Asfaw et al., 2018), and (3) stations across the study area are scarce (Alemayehu & Bewket 2017) and do not cover all of the study sites.

Data preparation and quality control

As needed for each analysis, daily data was averaged monthly, seasonally, and annually. RHtestsV3 and RHtests dlyPrp software tools were used to detect and account for erroneous shifts in climatic data series. Since these tests indicated no major change points or homogeneities requiring mean adjustments, the original data set was used for further analysis. serial autocorrelation was estimated using the autocorrelation function (acf package) in R statistical software (Kafadar et al., 2006).

Methods of data analysis

Rainfall and temperature variability were assessed by calculating coefficients of variation (CVs) at various time scales and mapping the CVs to examine their spatial patterns. Annual and seasonal rainfall and temperature variations were assessed using the standardized anomaly. The one-way ANOVA was applied to check whether the differences in the mean rainfall and temperature across the study districts were significantly different. Trend analyses were performed using the MK and ITA trend test techniques.

Innovative Trend Analysis (ITA)

The ITA technique was first suggested by Sen (2012) for the detection of time series trends. Unlike the MK trend test, the ITA technique does not consider any assumptions on the distribution and is unaffected by serial correlation or data length. It is simple to grasp and compute, and the results can be visually represented. In this method, the first step involves dividing the data into two halves and arranging them in increasing order. As an example, in the present study, there were 38 rainfall and temperature observations (1981–2018); hence, the first 19 observations were placed in the first half, and the next 19 observations were placed in the second half of the data. In the second procedure, the first half of the sub-series is placed on the X-axis of a Cartesian coordinate system, while the second half is placed on the Y-axis, as indicated in Figure 2. If the data points in a scatter plot fall above or below the bisector line at 1:1 (45°), the time series has an upward or downward trend (Sen, 2012). There would be no sign of a pattern if the data points were collected on the 1:1 line. In this paper, a 10% confidence band was applied to visualize the distance of points from the no-trend line. The purpose of this band is to enable the user to identify the distance between the points and the line of no-trend with no statistical interpretation (Caloiero, 2018; Nisansala, 2020).

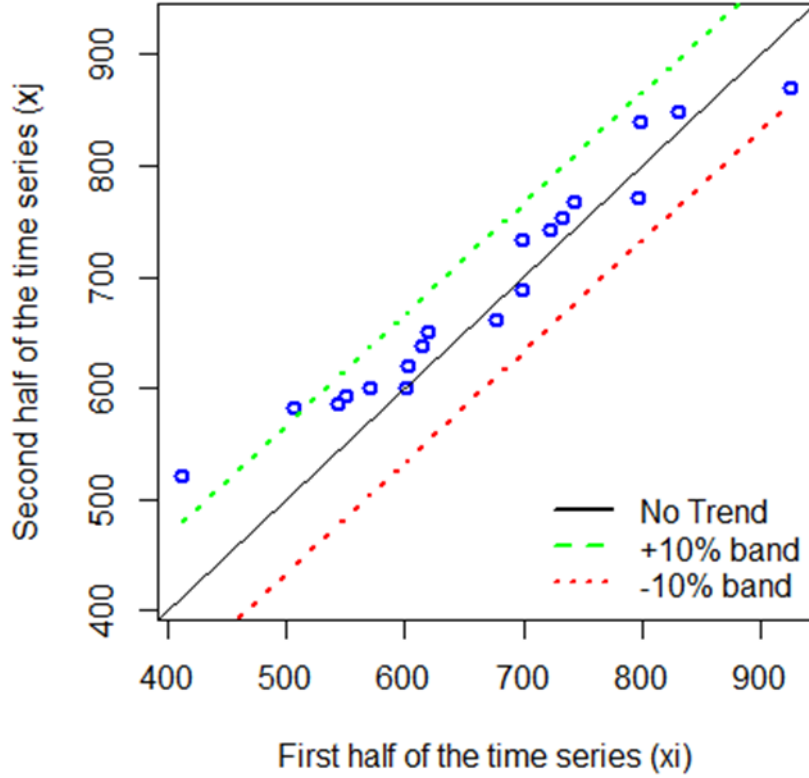


Figure 2. Illustration of the ITA technique (Sen, 2012). The 1:1 line is represented by the central black solid line (trendless). Broken green and red lines indicate confidence bands at +10% and -10%, respectively. A significant decreasing trend is shown by points below -10%, whereas a significant increasing trend is shown by points above +10%.

The actual value of the inconsistency between the y and x values is the distance from the 1:1 line (Nisansala 2020; Wu and Qian 2017), and the ITA trend pointer is derived by:

$$D = \frac{1}{n} \sum_{i=1}^n 10 \frac{(y_i - x_i)}{\underline{x}} \quad (1)$$

Where D is the trend, a positive D number represents an increasing trend, and a negative D number represents a decreasing trend; n denotes the number of subseries; and the first subseries' average. For comparison with the MK test, Equation (1) uses a multiplication factor of ten (Sen, 2012).

Mann-Kendall (MK) test

The MK (Kendall, 1975; Mann, 1945) is a non-parametric test that can be used with data that is not normally distributed. Because the statistic is based on the sign of differences rather than the actual values of the random variable, it is less affected by outliers. The trend statistic (S) of MK is obtained as:

$$S = \sum_{i=1}^{n-1} \sum_{j=k+1}^n (X_j - X_k) \quad (2)$$

Where X_k and X_j are timeseries data values k and j ($j > k$), n is the value of data points, and $(X_j - X_k)$ is given as:

$$(X_j - X_k) = \begin{cases} +1 & \text{if } (X_j - X_k) > 0 \\ 0 & \text{if } (X_j - X_k) = 0 \\ -1 & \text{if } (X_j - X_k) < 0 \end{cases} \quad (3)$$

The variance of Mann-Kendal's test is computed as:

$$(S) = \frac{n(n-1)(2n+5) - \sum_{p=1}^q t_p(t_p-1)(2t_p+5)}{18} \quad (4)$$

Where q is the number of tied groups and t_p is the number of data points in the p^{th} group. the summary of Equation (4) can be omitted if there are no ties.

The values of S and (S) are used to calculate the Z statistic:

$$Z = \begin{cases} \frac{S-1}{\sqrt{Var(S)}} & \text{if } S > 0 \\ 0 & \text{if } S = 0 \\ \frac{S+1}{\sqrt{Var(S)}} & \text{if } S < 0 \end{cases} \quad (5)$$

The MK test, in contrast, ignores this sequential correlation (Hamed and Rao, 1998). Because sequential association increases the possibility of identifying a notable trend when there is no significant trend, it might lead to a misunderstanding of the results. As a result, the modified MK test is used in this study, which takes all sequential correlations into consideration, as implemented in the R-package *modifiedmk*. When sequential autocorrelation was insignificant, a conventional set of tests (command *mktest*) was employed. However, when it was significant, the test was done using a technique described by Hamed (2009), which applies a bias correction when utilizing the same R package's pre-whitening (*bcpw*) tool.

Sen's slope estimator

The extent of the trend is frequently estimated by Sen's estimator because the MK test only detects trends (increasing or decreasing) (Sen, 1968). The extent of the trend is computed as:

$$Q_i = \frac{X_j - X_k}{j - k}, \quad \text{for } i = 1, 2, \dots, N, \quad (6)$$

Where X_j and X_k are data at time j and k ($j > k$), respectively. The median of N values of Q_i is shown as Sen's slope, which is computed as:

$$Q_i = \begin{cases} T_{\frac{N+1}{2}}, & \text{if } N \text{ is odd,} \\ \frac{1}{2} \left(T_{\frac{N}{2}} + T_{\frac{N+2}{2}} \right), & \text{if } N \text{ is even.} \end{cases} \quad (7)$$

When the number of N slope observations is odd, the Sen's estimator is obtained as "Qmed" = $(N+1)/2$, and for even times of observations, the slope is computed as "Qmed" = $[(N/2) + ((N+1)/2)]$. A positive slope indicates an upward trend, whereas a negative slope indicates a downward trend. There is no trend if the slope is 0.

RESULTS AND DISCUSSION

Rainfall

Temporal rainfall variability

The average annual rainfall was 971.3 mm, with a spatial variability of 788.8 mm in Simada and 1096.2 mm in Lay Gayint. *Kiremt* rainfall accounts for the largest portion of the study area (> 75%), followed by *Belg* rainfall, which contributes about 13% of the annual rainfall (Table

1). The coefficient of variability (CV) for annual rainfall ranged from 20.6% in Tach Gayint to 25.2% in Simada. *Belg* rainfall showed a high CV compared to *Kiremt* rainfall. Variability in seasonal rainfall has implications for farming practices in the area since the amount and quality of agricultural produce are determined by the onset, duration, and offset of rainfall. The result agrees with the findings of Alemayehu and Bewket (2017; Asfaw et al., 2018), who reported more variability in *Belg* rainfall than *Kiremt* rainfall in their respective study areas.

Table 1. Patterns of seasonal and annual rainfall

District	Parameter	Rainfall (mm)	Contribution to annual (%)	Coefficient of variation (CV, %)
Lay Gayint	Annual	1096.0	-	22.2
	<i>Kiremt</i>	746.4	76.1	15.4
	<i>Belg</i>	143.1	13.1	51.2
Tach Gayint	Annual	820.2	-	20.6
	<i>Kiremt</i>	622.7	78.2	14.9
	<i>Belg</i>	128.5	12.2	49.3
Simada	Annual	788.8	-	25.2
	<i>Kiremt</i>	596.8	73.2	17.5
	<i>Belg</i>	123.1	13.2	44.2

Note: $CV < 20\%$ = low variability; $20\% < CV < 30\%$ = medium variability; and $CV > 30\%$ = high variability (Alemu and Bawoke, 2020).

Figure 3 illustrates normalized seasonal and annual rainfall anomalies from long-term averages from 1981 to 2018. The percentage of negative deviations varies from 39% (Lay Gayint) to 65% (Simada) over the period of observation. Anomalies in seasonal rainfall exhibit similar distributions. Annual rainfall shows negative anomalies between 1981 and 1992 throughout the study area. Positive anomalies for *Kiremt* rainfall are observed in Simada for the period 1986-1996, except for the years 1987 and 1995. However, for the years 2003, 2005, 2006, and 2007, *Kiremt* rainfall showed negative anomalies from 1997 to 2013. *Kiremt* rainfall showed positive deviations for the period 1988-1995, except for the year 1987 in Tach Gayint. Likewise, positive anomalies in *Kiremt* rainfall were observed in Lay Gayint from 1988 to 1996 and 2007 to 2015, except for the year 2013. *Belg* rainfall showed high inter-annual variation over the period of observation. Negative and positive deviations for *Belg* rainfall accounted for 42% and 58% of the total in Lay Gayint and Tach Gayint, respectively. On the other hand, in Simada, positive and negative anomalies for *Belg* rainfall accounted for 34%

and 66%, respectively, over the period of observation. The majority of the historical drought occurrences in the study area correlate to the country's documented historical droughts.

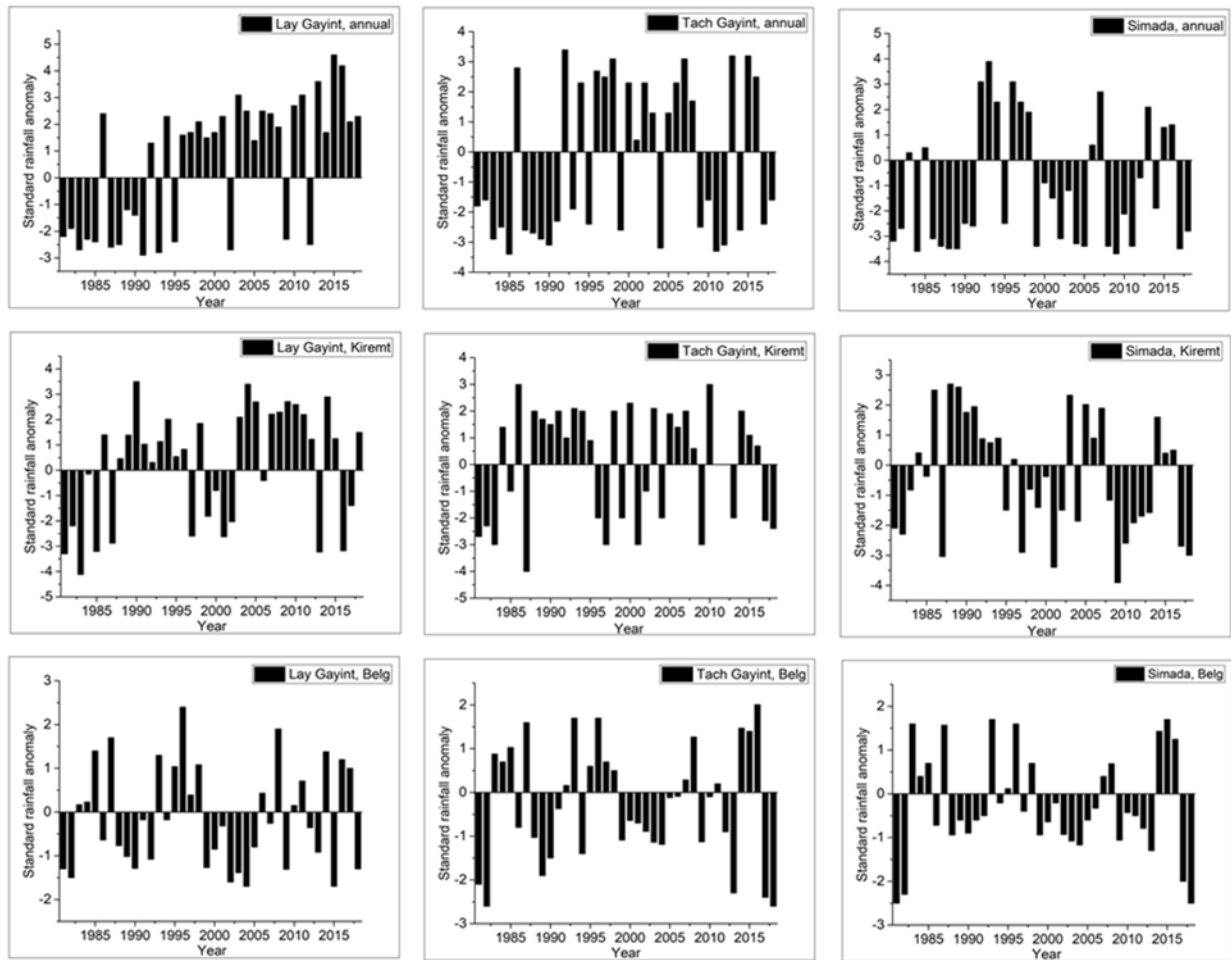


Figure 3. Annual and seasonal rainfall anomalies.

Rainfall trends

Seasonal, annual and rainfall trends are examined using the MK and ITA techniques (Table 2). Based on the MK test, annual rainfall exhibited a significant increasing trend (7.9 mm/year) in Lay Gayint at $p = 0.01$ level and an increasing trend (7.0 mm/year) in Tach Gayint at $p = 0.05$ level, but a non-significant, decreasing trend in annual rainfall was observed in Simada. At the seasonal level, *Kiremt* and *Belg* rainfall presented a non-significant upward trend in Lay Gayint and Tach Gayint. However, *Kiremt* and *Belg* rainfall revealed a non-significant downward trend in Simada. Similarly, a downward trend in *Kiremt* and *Belg* rainfall was informed by Alemayehu and Bewket (2017). Coupled with the long dry period from October to February (*Bega* season), the declining trend of *Belg* rainfall affects water and fodder availability for livestock in the study area.

Mann-Kendall's test and Sen's slope estimator indicated that July (3.4 mm/year) and August (2.9mm/year) rainfall exhibited a statistically significant increasing trend in Lay Gayint at $p = 0.05$ level. At $p = 0.05$ level, rainfall in Tach Gayint showed a significant increasing trend in August (1.9 mm/year) and November (0.4 mm/year). September rainfall in Simada (-0.9 mm/year) showed a significantly decreasing trend at $p = 0.05$ level over the study period.

Table 2. The MK and ITA trend test values of rainfall

Month	Lay Gayint			Tach Gayint			Simada		
	Z _{MK}	β	D	Z _{MK}	β	D	Z _{MK}	β	D
January	-0.46	0.00	-1.29	-0.63	-0.00**	-1.04	-0.83	-0.00	-2.72
February	-1.20	-0.10	-2.66	-1.77	-0.16	-4.45	-1.64	-0.03	-3.01
March	0.05	0.03	-0.32	-0.57	-0.16	-0.67	-0.42	-0.11	-0.65
April	0.54	0.25	0.16	0.50	0.18	-1.06	-1.10	-0.34	-2.32
May	0.88	0.53	0.02	0.70	0.46	0.02	0.21	0.16	-1.10
June	1.08	0.75	0.77	1.26	0.60	-0.75	0.20	0.11	-1.42
July	2.13	3.40**	1.66	1.45	1.82	1.15	-0.21	-0.37	-1.01
August	2.43	2.98**	2.74	1.96	1.90**	1.70	0.95	1.15	0.12
September	1.30	0.62	1.56	-0.15	-0.04	0.04	-2.23	-0.90**	-1.73
October	-0.01	0.00	-3.09	0.26	0.05	-1.63	0.06	0.03	-2.30
November	1.78	3.44	3.05	2.21	0.36**	3.77	1.76	0.30	2.67
December	-0.60	-0.01	-0.81	-0.19	-0.00	-0.33	-0.24	-0.00	-3.11
<i>Belg</i>	1.43	1.56	1.90	0.12	0.21	0.77	-0.31	-0.37	-1.48
<i>Kiremt</i>	1.88	7.45	1.72	0.77	1.95	0.57	-1.33	-3.08	-1.22
Annual	2.73	7.89***	1.02	2.47	7.00**	1.13	-0.47	-0.78	-0.52

*, **, and *** are significant at alpha values of 0.1, 0.05, and 0.01, respectively.

Z_{MK}, standardized MK; β , Sen's slope; D, trend indicator of ITA.

Table 2 presents trend analysis using the ITA technique. It is shown that mean seasonal, and annual rainfall mostly exhibited positive D values. The majority of annual rainfall data at Lay Gayint and Tach Gayint fell beyond the 1:1 line, as shown in Figure 4, indicating an increasing trend within the +10% confidence band, but most of the data points in Simada fell below the 1:1 line, showing a downward trend in annual rainfall within the -10% confidence band over the period of observation. For the *Kiremt* rainfall, most of the data points were above the +10% confidence band parallel to the 1:1 line in Lay Gayint and Tach Gayint, indicating a significant increasing trend, whereas most of the data points were within the +10% confidence band parallel to the 1:1 line, showing an increasing tendency for *Kiremt* rainfall for Simada. Belg rainfall indicated a downward trend in Tach Gayint and Simada, but an unclear trend in Lay Gayint.

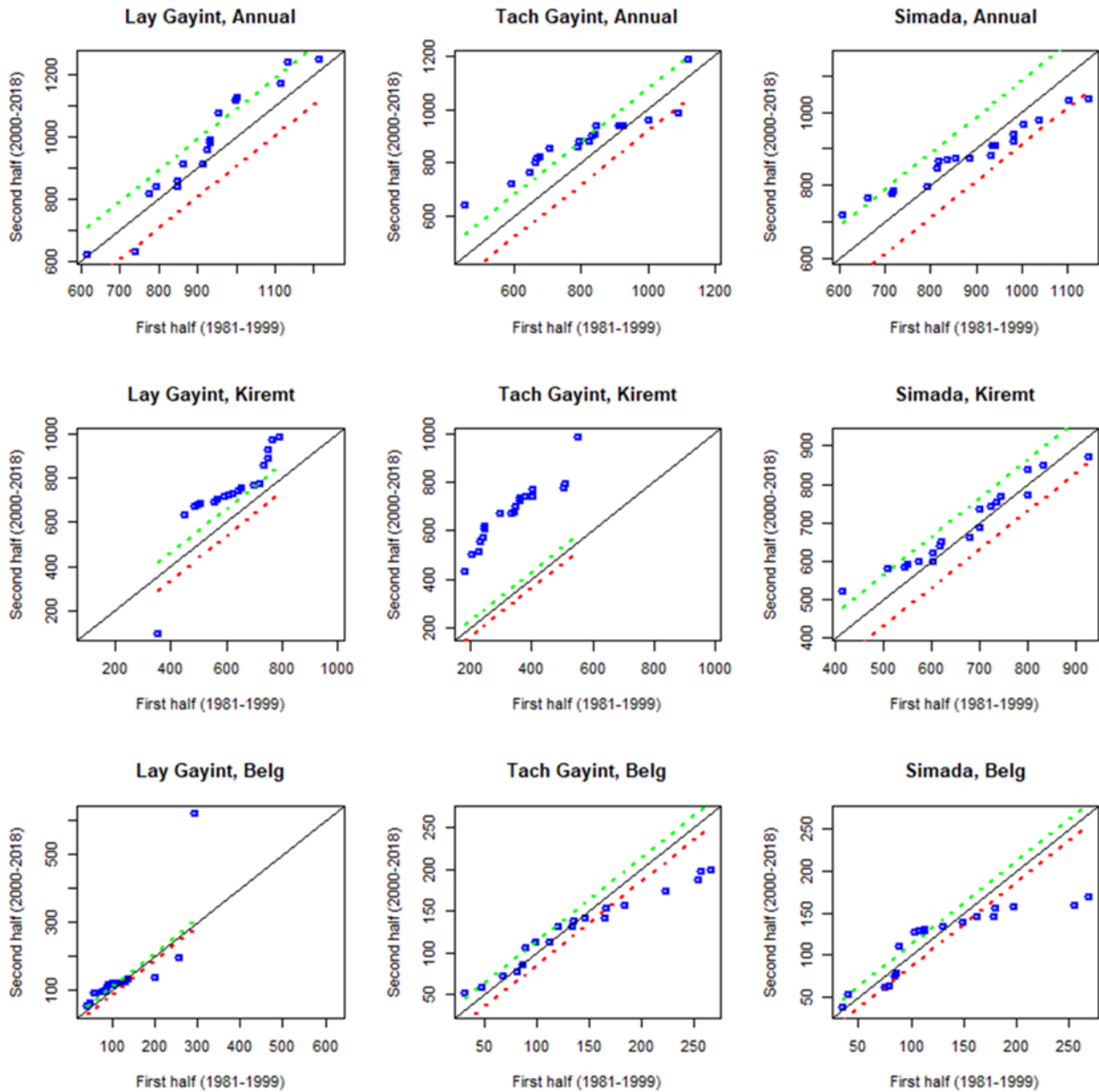


Figure 4. Annual and seasonal rainfall trends using ITA technique.

The results of ITA for mean monthly rainfall are shown in (Figures 5–7). A significant increasing trend was found in Lay Gayint in June, July, August, and September (*Kiremt* season) and November, but March, April, and May (*Belg* season) showed mixed increasing and decreasing trends (Figure 5). In Tach Gayint, a negative trend was found for all months except June, July, August, and November (Figure 6). In Simada, all months showed decreasing trends except June, August, and November (Figure 7).

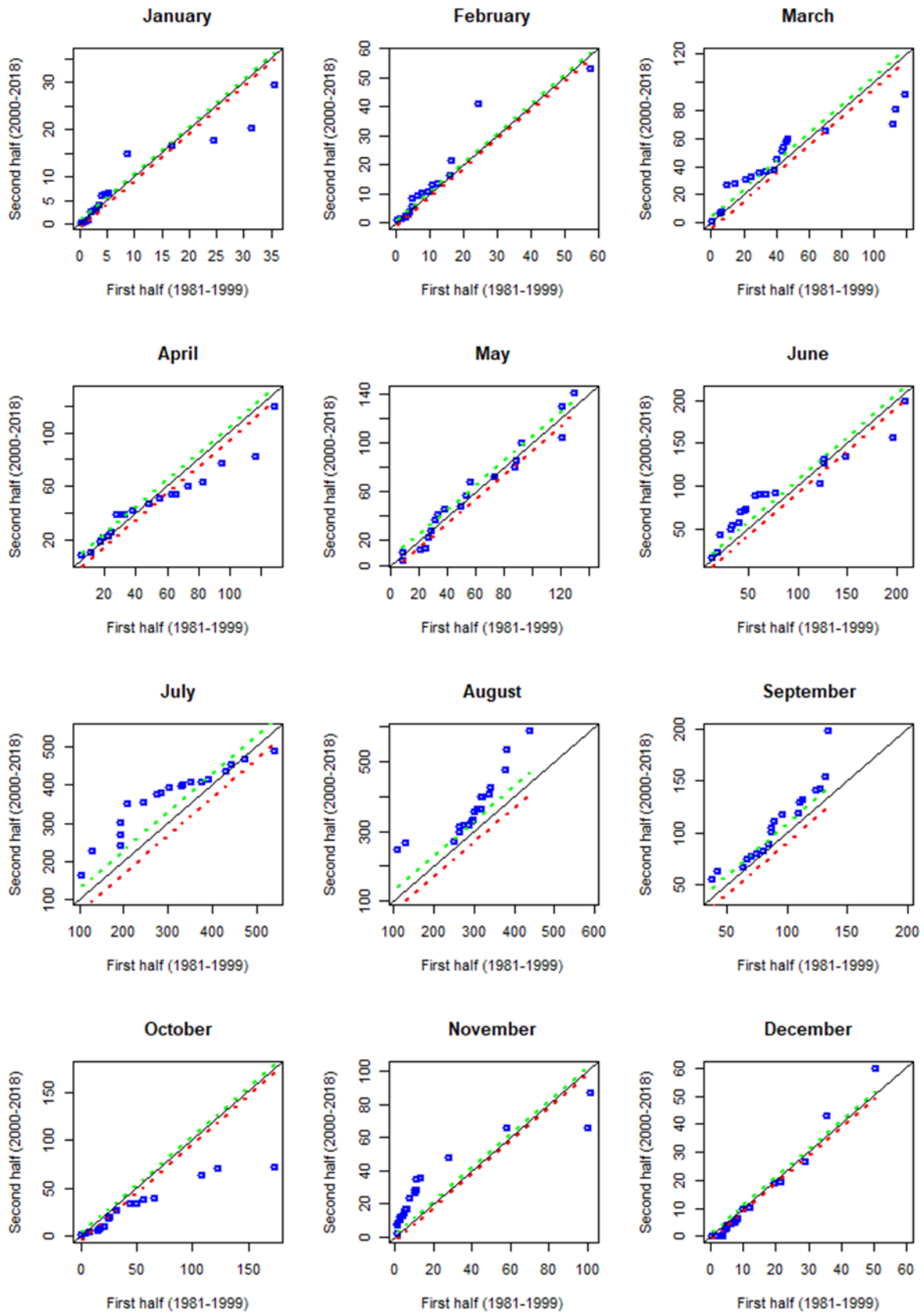


Figure 5. Mean monthly rainfall trends in Lay Gayint using ITA method.

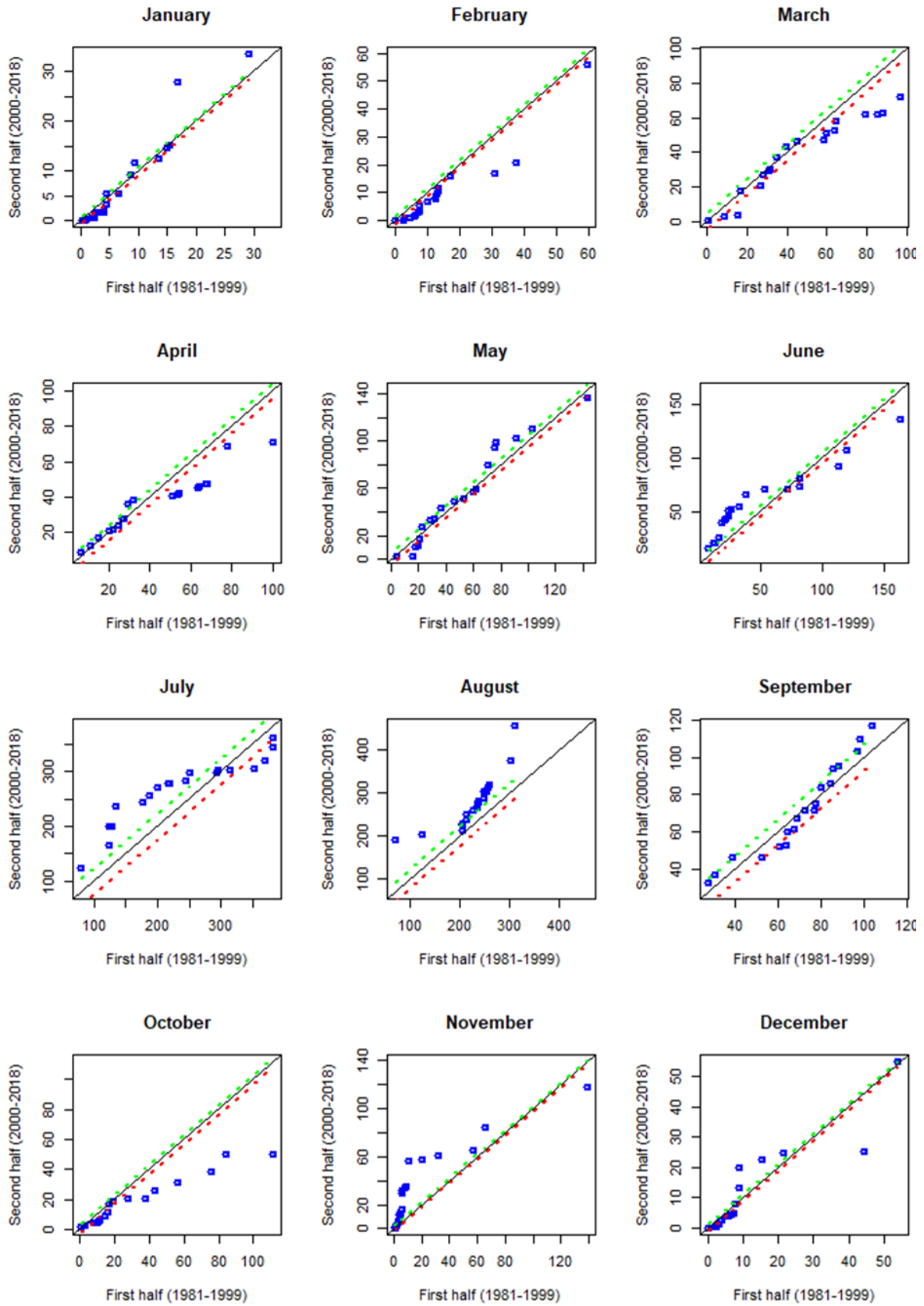


Figure 6. Mean monthly rainfall trends in Tach Gayint using ITA method.

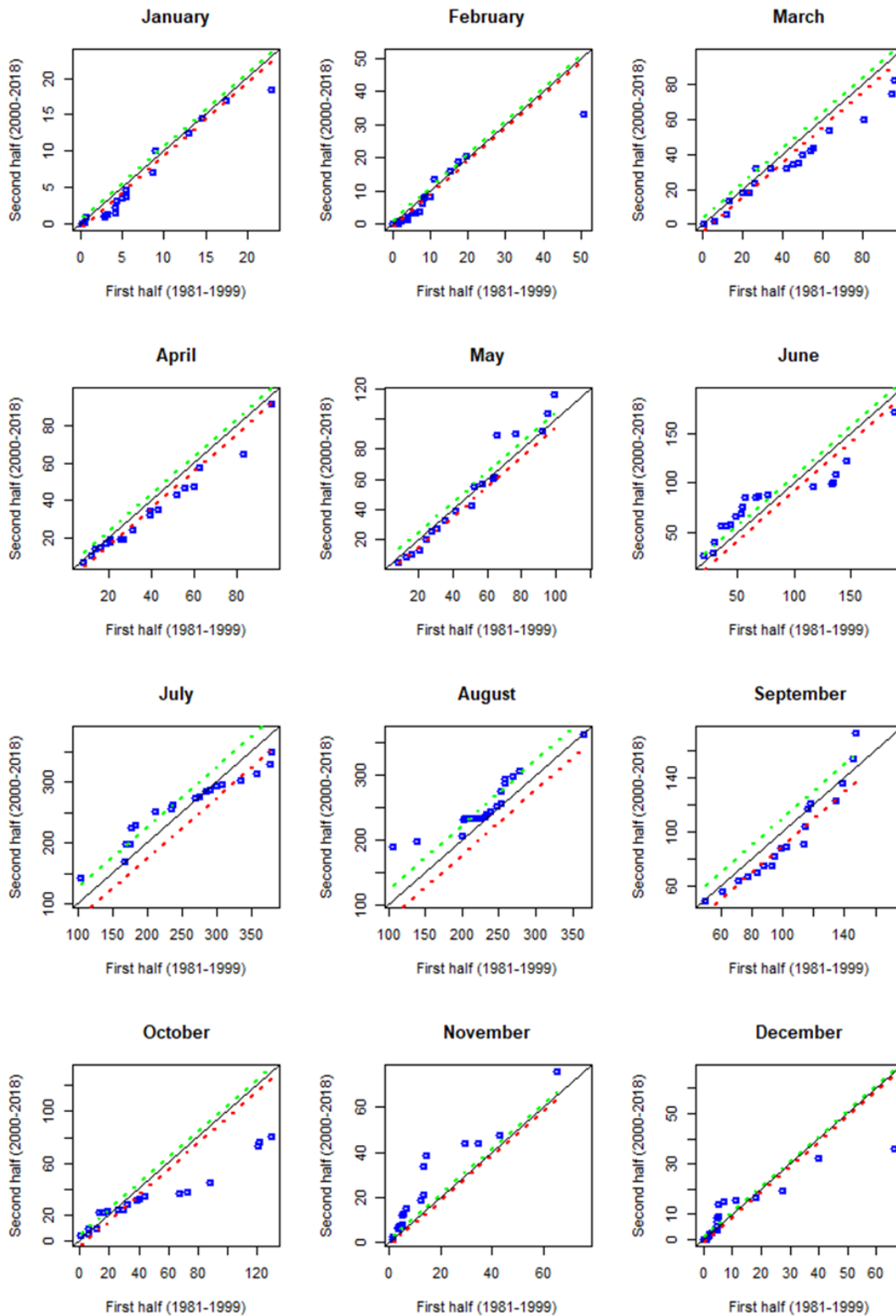


Figure 7. Mean monthly rainfall trends in Simada using ITA method.

Spatial variability of rainfall

Seasonal and annual rainfall showed considerable spatial variation. The western part receives a higher amount of rainfall than the eastern part (Figure 8). Lay Gayint gets 760 to 860 mm of rainfall per year in 46% of the area. Annual rainfall ranges from 861 to 961 mm in 30% of the

area and 962-1200 mm in the remaining 24%, respectively. Tach Gayint receives annual rainfall ranging from 760 to 860 mm in about 78% of the area, while the remaining 22% receives annual rainfall ranging from 861 to 961 mm. Simada receives annual rainfall ranging from 760 to 860 mm in approximately 82% of the area. More than 48% of Lay Gayint receives *Kiremt* rainfall between 550 and 750 mm. A *Kiremt* rainfall ranging from 550 to 750 mm falls on a large portion of Tach Gayint (85%). More than 89% of Simada receives *kiremt* rainfall between 550 and 750 mm. In Tach Gayint, nearly 57% of the area receives *Belg* rain of between 40 and 100 mm. A large part of Simada (68%) receives *Belg* rainfall between 40 and 100 mm. One-way ANOVA showed that annual and *kiremt* rainfall significantly varied at a $p = 0.01$ level among the three districts. The Tukey's post-hoc mean evaluation indicated that mean annual rainfall in Lay Gayint was higher by 243 mm than in Tach Gayint and by 204 mm in Simada at a $p = 0.01$ level. As shown in Table 3, the amount of *Kiremt* rainfall in Lay Gayint is 220 mm higher than in Tach Gayint and 172 mm in Simada, at $p = 0.01$ and $p = 0.05$ levels, as shown in (Table 3), whereas the mean annual and *Kiremt* rainfall did not show significant variation between Tach Gayint and Simada.

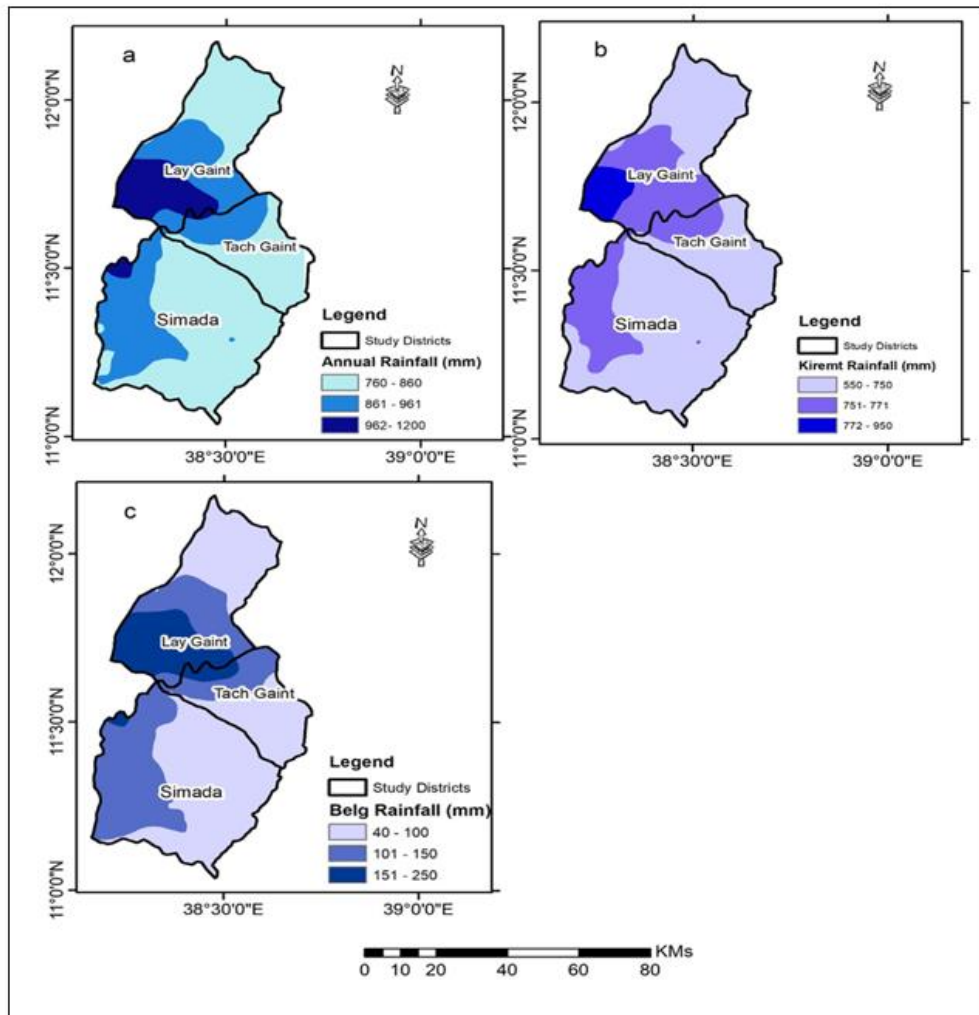


Figure 8. Spatial distribution of rainfall.

Table 3. ANOVA and Tukey's post hoc comparison test. (I) and (J) refer to the two districts being compared in each case.

Mean difference (I-J)			
(I) District	(J) District	Annual rainfall	Kiremt rainfall
Lay Gayint	Tach Gayint	243.66***	220.83***
	Simada	204.23***	172.21**
Tach Gayint	Simada	-39.42	-48.62
ANOVA <i>F</i> -ratio		22.91***	20.35***

** and *** are significant at alpha values of 0.05 and 0.01, respectively.

The spatial distribution of coefficient variation (CV) of rainfall is shown in (Figure 9). Annual and *Kiremt* rainfall exhibited relatively similar coefficients of variation (CV) across the study area. As rainfall is relatively abundant in the *Kiremt* season, the CV is generally low across the area. The CV is the smallest in the high-elevation district (Lay Gayint).

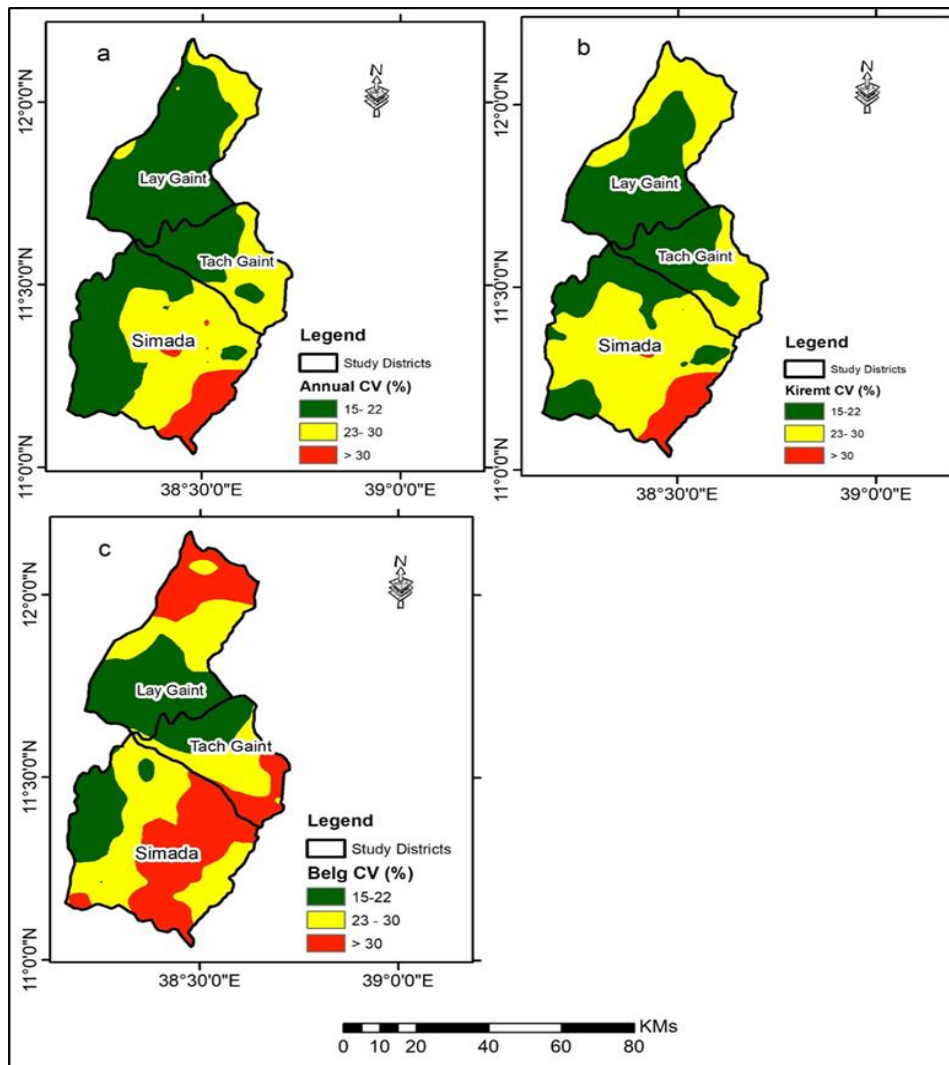


Figure 9. Spatial distribution of the coefficient of variation for rainfall.

Temperature

Temporal variability of temperature

The mean annual temperature ranges from 14.4°C in Lay Gayint to 18.2°C in Simada (Figure 10). The highest monthly temperature for Lay Gayint is 22.2°C (March) and its lowest is 6.5°C (December). The highest and lowest values for Simada are 25.1°C (March) and 8.0°C (December), respectively. The highest temperature recorded for Tach Gayint is 22.7°C (March) and the lowest is 6.6°C (December).

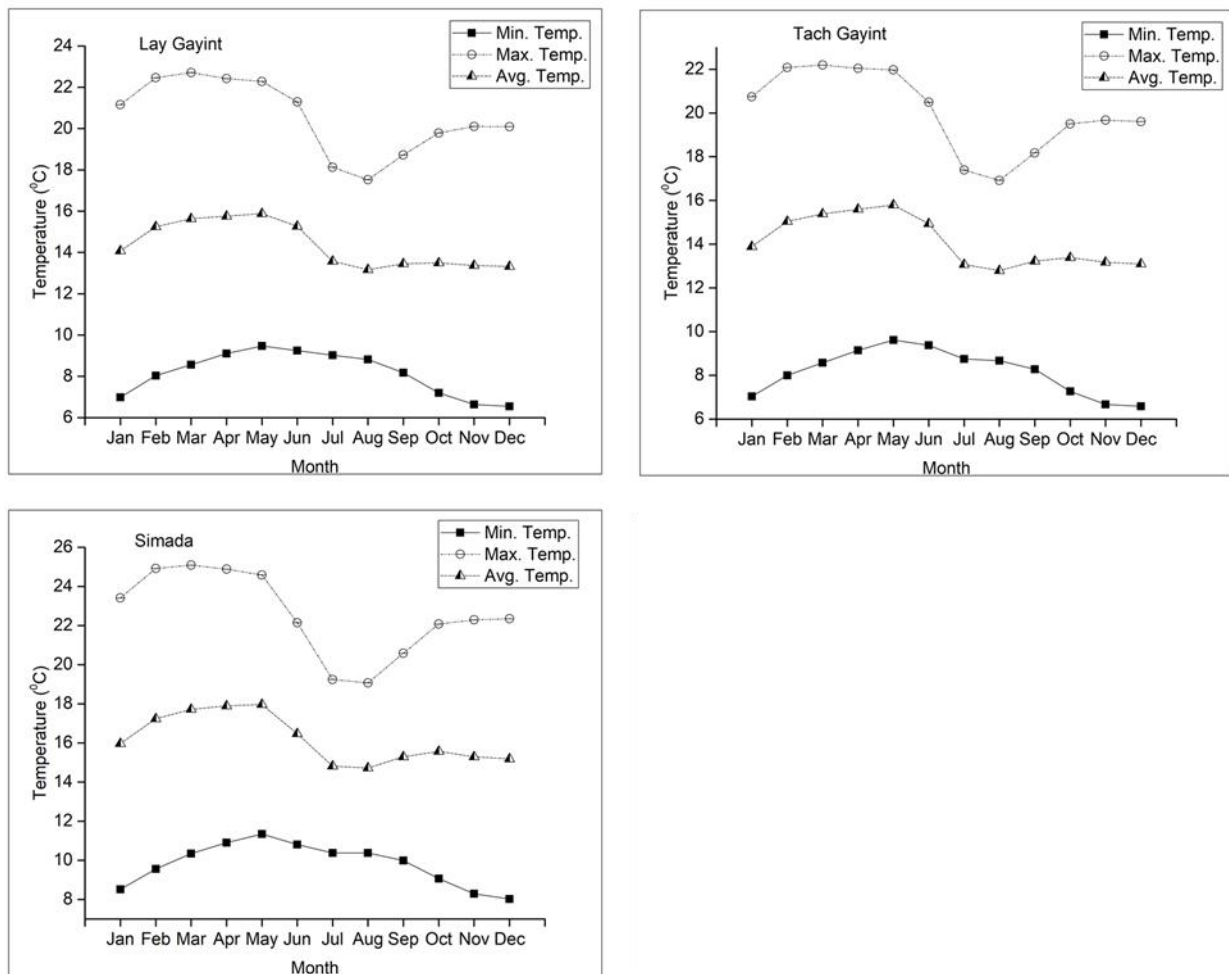


Figure 10. Mean monthly temperature distribution.

Figures 11 and 12 show the variation in mean annual maximum and minimum temperatures yearly. The decade of the 2000s was found to be warmer than the 1980s and 1990s. The seasonal anomalies in maximum and minimum temperatures follow the same trends as the mean annual maximum and minimum temperatures. The 2000s were warmer than the preceding decades in all seasons.

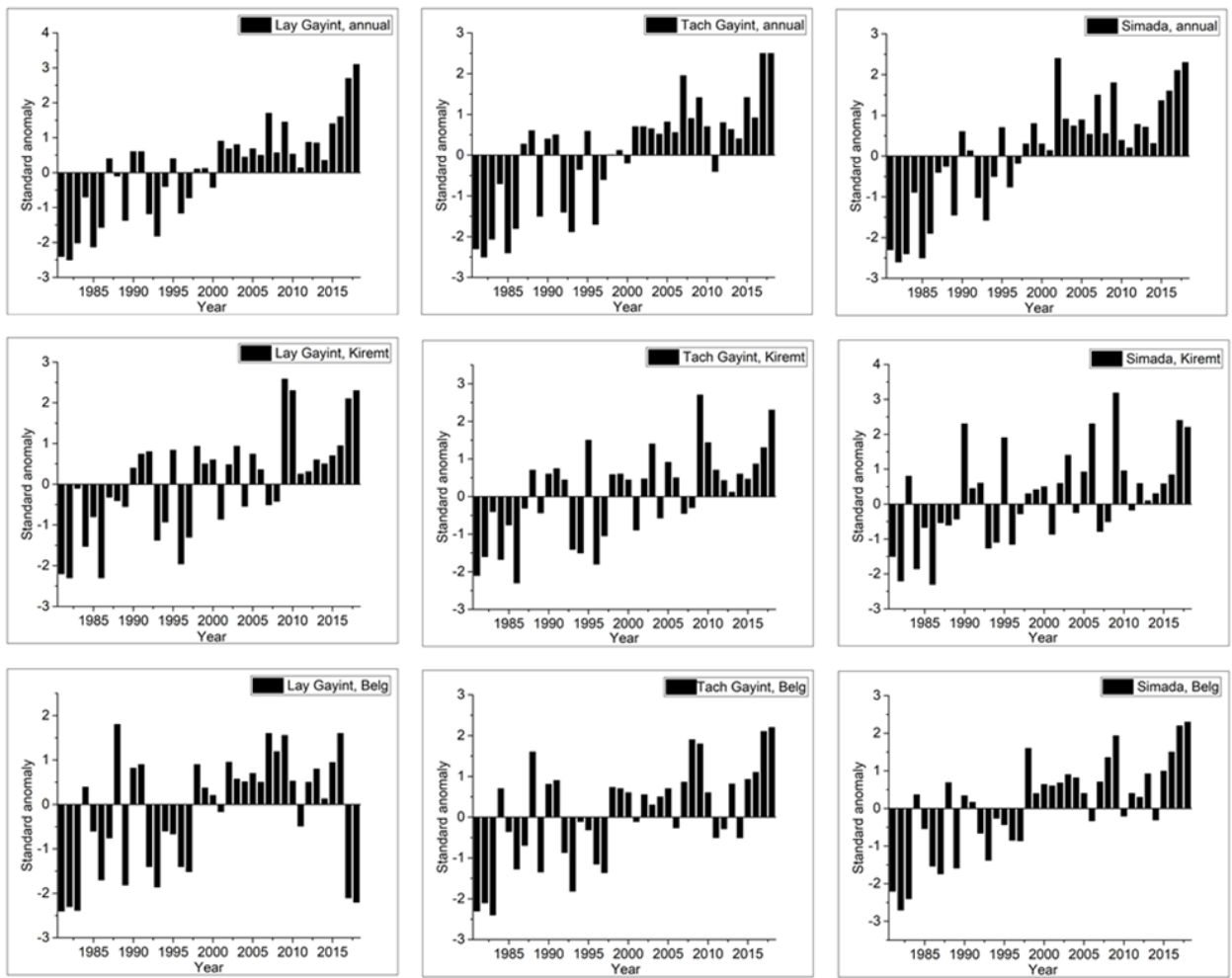


Figure 11. Anomaly in temporal and spatial variation in the mean maximum temperature.

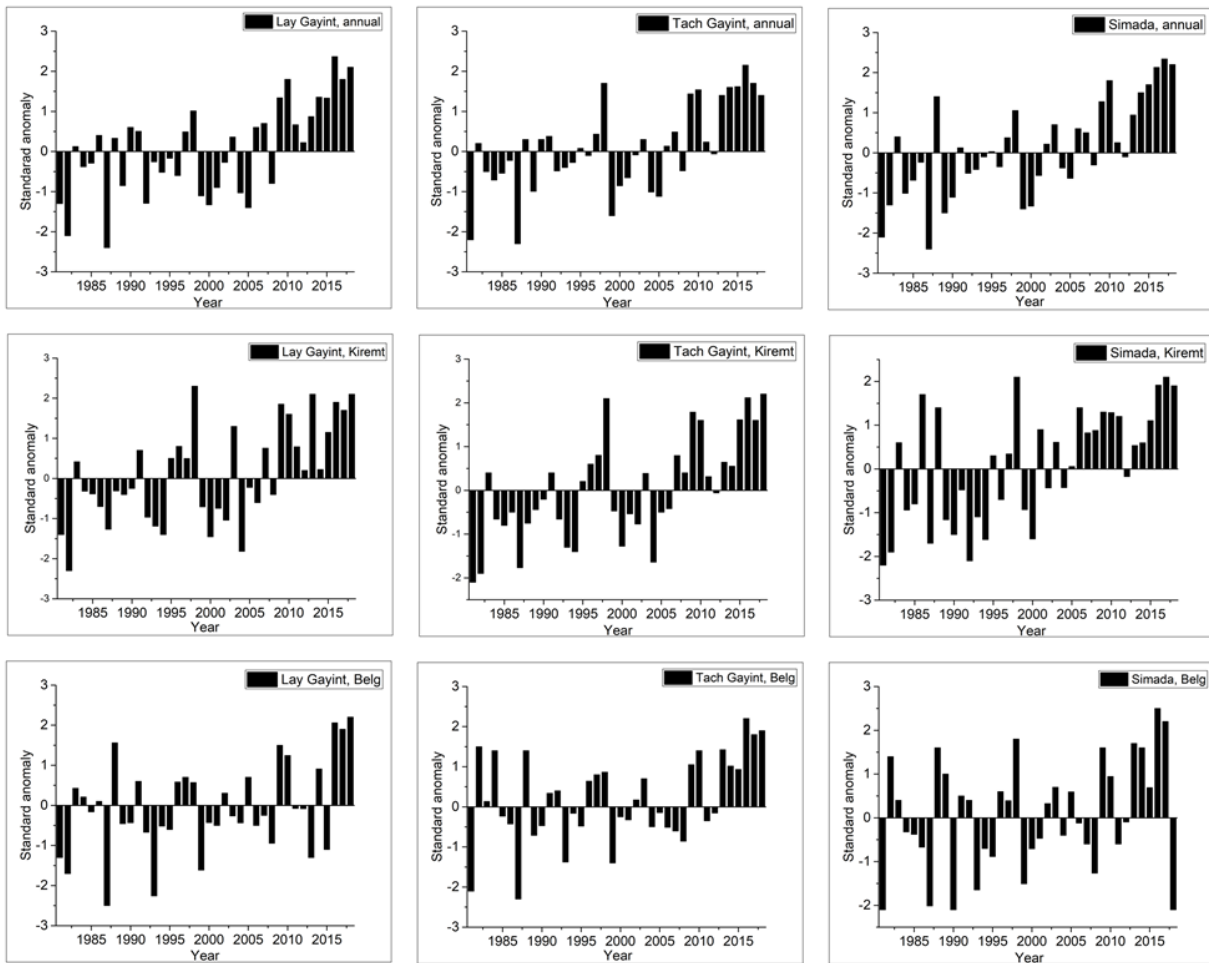


Figure 12. Anomaly in temporal and spatial variation in the mean minimum temperature.

Temperature trends

Similar to rainfall trend analysis, annual and seasonal temperature trends were assessed by ITA and MK techniques. The MK's trend test showed annual *Kiremt* and *Belg* minimum temperatures to have experienced significant warming trends in Simada and Lay Gayint at a $p = 0.05$ level (Table 4).

Our findings coincide with the results reported by Ademe et al. (2020), Alemayehu and Bewket (2017), Asfaw et al. (2018), Belihu et al. (2018), and Gebrehiwot et al. (2019), where significant warming trends in mean annual minimum temperatures were described for different parts of Ethiopia. Our findings differ from the findings of Alemayehu and Bewket (2017) and Asfaw et al. (2018), who reported that the minimum temperature had increased substantially more in recent years than the maximum. However, other studies, for instance, Ademe et al. (2020), Berhane et al. (2020) and Kahsay et al. (2019) agree with the findings of the present study, which found an increase in the maximum temperature has increased substantially more in recent years than the minimum. The ITA technique showed an overall warming trend of mean annual and seasonal minimum temperatures (Table 4; Figure 13). The ITA's results for seasonal minimum temperatures (not shown here) were similar to the mean annual minimum temperature.

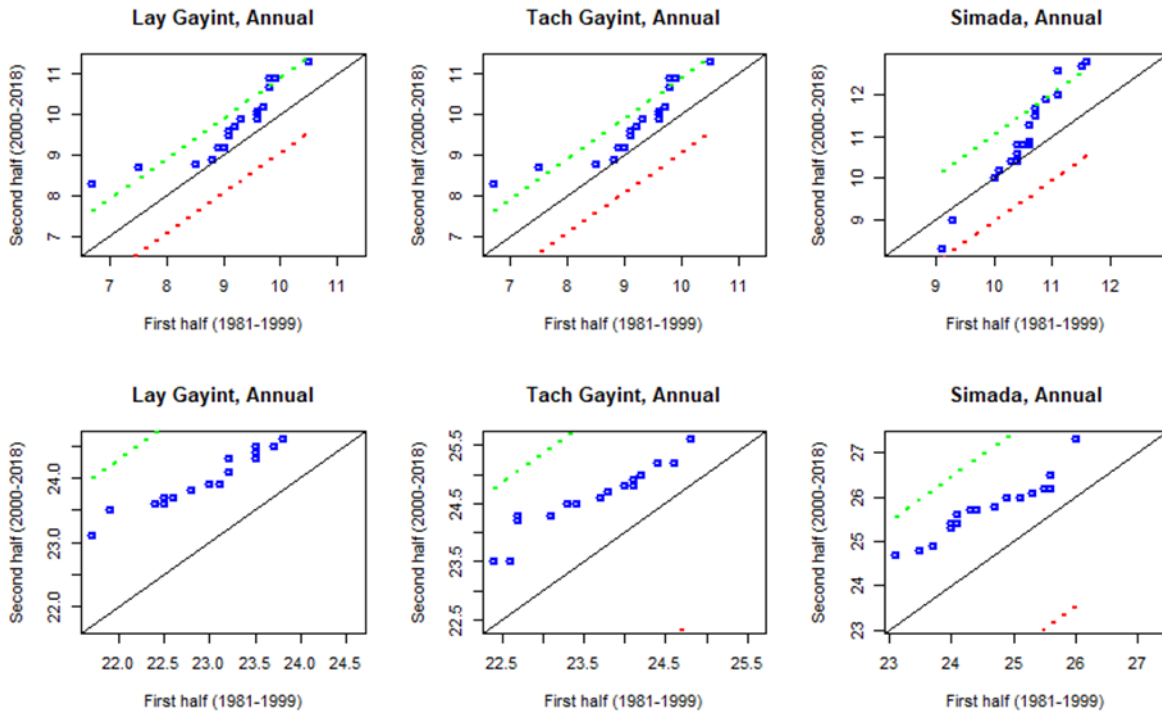


Figure 13. ITA technique for annual mean minimum (above) and maximum (below) temperatures.

Table 4. MK and ITA trend test values of mean minimum temperature at seasonal and annual timescales.

Month	Lay Gayint			Tach Gayint			Simada		
	Z_{MK}	β	D	Z_{MK}	β	D	Z_{MK}	β	D
January	0.54	0.01	0.37	0.34	0.00	0.85	0.87	0.01	0.60
February	1.05	0.02	1.12	1.84	0.02	0.93	2.45	0.04**	0.89
March	0.88	0.01	1.09	0.31	0.00***	0.76	2.10	0.04**	0.79
April	2.57	0.03**	0.95	0.87	0.01	0.64	2.72	0.04***	0.62
May	3.13	0.05***	0.98	1.92	0.02**	0.74	1.83	0.03**	0.47
June	3.40	0.05***	1.02	3.12	0.03***	0.59	1.28	0.01**	0.25
July	3.23	0.04***	0.74	2.09	0.02**	0.23	1.66	0.02	0.24
August	2.65	0.04***	0.66	1.88	0.02	0.20	0.56	0.01**	0.12
September	1.90	0.02**	0.42	1.97	0.03**	0.21	1.78	0.02	0.14
October	1.82	0.03	0.09	1.58	0.03	0.06	1.35	0.03	0.33
November	2.03	0.04**	0.37	1.90	0.04**	0.50	0.67	0.01	0.36
December	0.52	0.01	-0.05	1.68	0.03	0.58	0.94	0.02	0.46
<i>Belg</i>	2.02	0.02**	1.01	1.29	0.01	0.73	2.79	0.04**	0.62
<i>Kiremt</i>	2.26	0.02**	0.73	1.50	0.01	0.30	1.44	0.02**	0.17
Annual	1.56	0.01**	0.67	1.19	0.01	0.55	2.01	0.02**	0.44

*, **, and *** are significant at alpha values of 0.1, 0.05, and 0.01, respectively
 Z_{MK} , standardized MK; β , Sen's slope; D , trend indicator of ITA.

Based on the Mk test, the trend of seasonal and annual maximum temperatures exhibited considerable warming tendencies at a $p = 0.01$ level. Moreover, the mean monthly maximum

temperature shows a statistically significant warming trend at the $p = 0.01$ level across the study area, except for June, July and November (Table 5).

Our findings coincide with those of Ademe et al. (2020), Alemayehu and Bewket (2017), Gebrehiwot et al. (2019) and Kahsay et al. (2019), where a significant warming trend in the mean annual maximum temperature was exhibited in their study areas. The result of the ITA technique revealed an overall warming trend in the mean maximum temperature in the area, as shown in (Table 5). The graphical results of the ITA technique revealed that most of the temperature data points fell above the 1:1 line, implying a warming trend of the mean annual maximum temperature with respect to a +10% confidence band parallel to the 1:1 line in the study area (Figure 13). The results (not presented here) of the ITA for seasonal and monthly maximum temperatures are similar to the mean annual maximum temperature.

Table 5. MK and ITA trend test values of mean maximum temperature at seasonal and annual timescales.

Month	Lay Gayint			Tach Gayint			Simada		
	Z_{MK}	β	D	Z_{MK}	β	D	Z_{MK}	β	D
January	2.09	0.02**	0.31	0.51	0.00	0.37	2.95	0.03****	0.47
February	3.20	0.05****	0.53	1.05	0.02	1.12	2.91	0.04****	0.63
March	3.19	0.05****	0.45	2.99	0.05****	1.09	3.54	0.06****	0.55
April	2.70	0.05****	0.51	3.80	0.05****	0.95	3.76	0.09****	0.70
May	2.21	0.05**	0.61	3.13	0.05**	0.98	2.21	0.04**	0.59
June	1.22	0.03	0.37	3.40	0.05****	1.02	1.72	0.04	0.24
July	1.87	0.02	0.20	3.23	0.04****	0.74	2.17	0.03**	0.25
August	3.22	0.03****	0.32	2.65	0.04****	0.66	2.17	0.03**	0.22
September	2.85	0.03****	0.22	1.90	0.05**	0.42	2.93	0.04****	0.30
October	3.76	0.06****	0.61	1.13	1.72****	0.09	2.49	0.04**	0.55
November	3.51	0.04****	0.56	1.64	0.03**	0.37	1.79	0.03	0.51
December	3.62	0.04****	0.50	0.11	0.03**	-0.05	2.78	0.04**	0.52
<i>Belg</i>	3.26	0.05****	0.51	3.61	0.05****	1.01	3.80	0.07****	0.62
<i>Kiremt</i>	3.20	0.03****	0.28	3.00	0.03****	0.73	2.53	0.03**	0.25
Annual	4.09	0.03****	0.44	1.56	0.01	0.67	2.31	0.02**	0.47

*, **, and **** are significant at alpha values of 0.1, 0.05, and 0.01, respectively

Z_{MK} , standardized MK test; β , Sen's slope; D , trend pointer of ITA.

Spatial variability of temperature

The north-eastern portions experience relatively lower temperatures than the south-western portions (Figure 14) due to the influence of climatic controls such as elevation. The one-way ANOVA showed that mean annual minimum and maximum temperatures significantly varied at a $p = 0.001$ level among the three districts. The mean minimum temperature in Simada was 1.3°C and 0.2°C higher than in Lay Gayint and Tach Gayint, respectively (significant at $p = 0.01$), and the mean minimum temperature in Tach Gayint was higher by 1.0°C than in Lay Gayint (significant at $p = 0.01$). At $p = 0.01$, Simada had a 1.0°C higher mean maximum temperature than Tach Gayint, and Tach Gayint had a 0.7°C higher mean maximum temperature than Lay Gayint (both significant at $p = 0.01$) (Table 6).

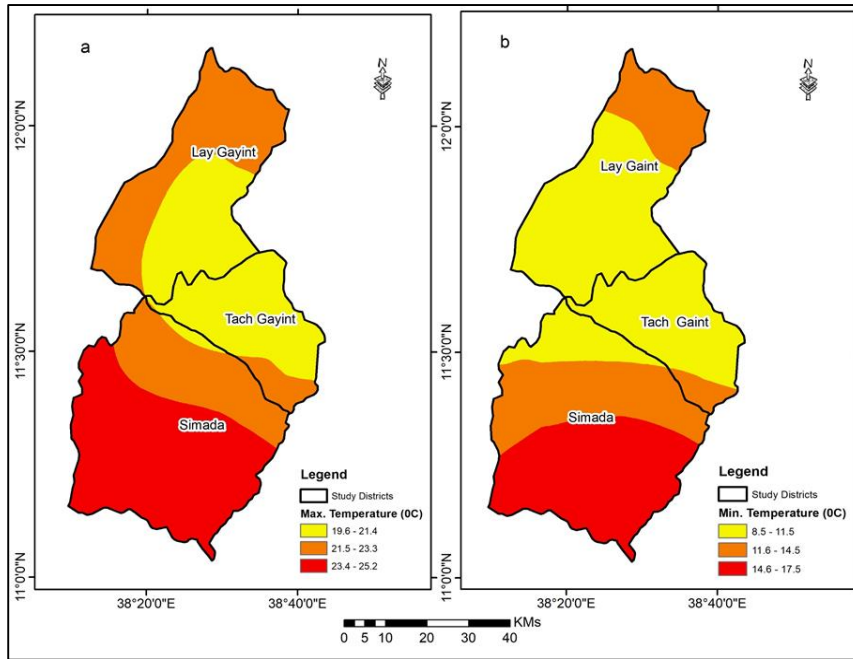


Figure 14. Spatial distribution of mean maximum (left) and mean minimum (right) temperature.

Table 6. ANOVA and Tukey's post hoc comparison for temperatures.

(I) District	(J) District	Mean difference (I-J)	
		Minimum Temp.	Maximum Temp.
Lay Gayint	Tach Gayint	-1.02***	-0.71***
	Simada	-1.26***	-1.73
Tach Gayint	Simada	-0.24***	-1.02***
ANOVA <i>F</i> -ratio		19.27***	43.62***

** and *** are significant at alpha values of 0.05 and 0.01, respectively.

Comparison of ITA and MK techniques

The reliability of the ITA technique was assessed by comparing its results with those of the MK trend test. Table 7 presents a summary and comparison of the Z values of the MK test and the D statistic of the ITA technique for monthly, seasonal, and annual rainfall and minimum and maximum temperatures. It is shown that most of the trends sensed by the MK test (in 28 time series, the result was positive, while in 20 time series, the result was negative) were also identified by the ITA (in 23 time series, the result was positive, whereas in 25 time series, the result was negative) (Table 7). However, both the ITA and MK tests detected positive trends for monthly, annual, and seasonal temperatures. But, the ITA method was found to have some advantages as it identified some hidden trends that might not have been identified by the MK test. Also, it overcomes assumptions about, for instance, the length of records, the normality of the distribution, and the independent structure of the time series (Wu and Qian, 2017). But, the ITA technique does not allow the determination of whether the variations between each point and the 1:1 line are significant. Therefore, we used a +10% confidence band to detect trends.

Table 7. Comparison of values of Z of MK test and statistics D of ITA method for rainfall and temperature.

<u>Temperature</u>	<u>Rainfall</u>				<u>Minimum Temperature</u>			<u>Maximum</u>	
	Lay Gayint Simada	Tach Gayint		Simada	Lay Gayint	Tach Gayint	Simada	Lay Gayint	
Tach Gayint	Z_{MK}/D	Z_{MK}/D	Z_{MK}/D	Z_{MK}/D	Z_{MK}/D	Z_{MK}/D	Z_{MK}/D	Z_{MK}/D	
Month	Z_{MK}/D	Z_{MK}/D	Z_{MK}/D	Z_{MK}/D	Z_{MK}/D	Z_{MK}/D	Z_{MK}/D	Z_{MK}/D	
January	-0.46/-1.29	-0.63/-1.04	-0.83/-2.72	0.54/0.37	0.34/0.85	0.87/0.60	2.09/0.31	0.51/0.37	2.95/0.47
February	-1.20/-2.66	-1.77/-4.45	-1.64/-3.01	1.05/1.12	1.84/0.93	2.45/0.89	3.20/0.53	1.05/1.12	2.91/0.63
March	0.05/-0.32	-0.57/-0.67	-0.42/-0.65	0.88/1.09	0.31/0.76	2.10/0.79	3.19/0.45	2.99/1.09	3.54/0.55
April	0.54/0.16	0.50/-1.06	-1.10/-2.32	2.57/0.95	0.87/0.64	2.72/0.62	2.70/0.51	3.80/0.95	3.76/0.70
May	0.88/0.02	0.70/0.02	0.21/-1.10	3.13/0.98	1.92/0.74	1.83/0.47	2.21/0.61	3.13/0.98	2.21/0.59
June	1.08/0.77	1.26/-0.75	0.20/-1.42	3.40/1.02	3.12/0.59	1.28/0.25	1.22/0.37	3.40/1.02	1.72/0.24
July	2.13/1.66	1.45/1.15	-0.21/-1.01	3.23/0.74	2.09/0.23	1.66/0.24	1.87/0.20	3.23/0.74	2.17/0.25
August	2.43/2.74	1.96/1.70	0.95/0.12	2.65/0.66	1.88/0.20	0.56/0.12	3.22/0.32	2.65/0.66	2.17/0.22
September	1.30/1.56	-0.15/0.04	-2.23/-1.73	1.90/0.42	1.97/0.21	1.78/0.14	2.85/0.22	1.90/0.42	2.93/0.30
October	-0.01/-3.09	0.26/-1.63	0.06/-2.30	1.82/0.09	1.58/0.06	1.35/0.33	3.76/0.61	1.13/0.09	2.49/0.55
November	1.78/3.05	2.21/3.77	1.76/2.67	2.03/0.37	1.90/0.50	0.67/0.36	3.51/0.56	1.64/0.37	1.79/0.51
December	-0.60/-0.81	-0.19/-0.33	-0.24/-3.11	0.52/-0.05	1.68/0.58	0.94/0.46	3.62/0.50	0.11/-0.05	2.78/0.52
<i>Bega</i>	-0.86/1.50	0.07/9.19	0.17/0.70	0.82/0.36	1.32/0.60	1.24/0.55	3.91/0.51	0.82/0.36	1.88/0.54
<i>Belg</i>	1.43/1.90	0.12/0.77	-0.31/-1.48	2.02/1.01	1.29/0.73	2.79/0.62	3.26/0.51	3.61/1.01	3.80/0.62
<i>Kiremt</i>	1.88/1.72	0.77/0.57	-1.33/-1.22	2.26/0.73	1.50/0.30	1.44/0.17	3.20/0.28	3.00/0.73	2.53/0.25
Annual	2.73/1.02	2.47/1.13	-0.47/-0.52	1.56/0.67	1.19/0.55	2.01/0.44	4.09/0.44	1.56/0.67	2.31/0.47

Potential implication of temperature and rainfall variability

Rainfall and temperature changes can have a wide range of implications for crop production and agricultural practices. Agricultural practices require adequate and timely rainfall amounts and duration throughout the *Belg* and *Kiremt* seasons. The irregularity and variability of rainfall during the *Kiremt* and *Belg* seasons, on the other hand, hinder farming activities and reduce production in the study area. In the northeastern highlands of Ethiopia, Mekonnen and Berlie (2020) found that the variability and irregularity of rainfall during the *Kiremt* and *Belg* seasons discourage farming practices and reduce production. Farmers' enthusiasm for early and timely planting, active growing, and maturation of various crops was influenced by delayed onset of rainfall in February and the cessation of rainfall in September. Alemayehu and Bewket (2016) and Bewket (2009) also stated that climate variability and changes have a substantial influence on food security and crop production in the north-central highlands and Amhara region, respectively. An increase in temperature could have a distinct impact on crop production (Pachauri et al., 2014). This might be due to invasive plants and crop pests that appear at different times during the agricultural calendar (EPCC 2015; Mekonnen and Berlie, 2020). Temperature fluctuations have also had an impact on pasture and forage production, as well as caused animal diseases (Gebreegziabher et al., 2020). Generally, when climate variability reaches its peak, it causes total crop failure, resulting in starvation and the deaths of people and animals. These circumstances are common in different parts of Ethiopia.

CONCLUSION

Temperature and rainfall data from 1981 to 2018 were analysed using various meteorological indices to highlight spatiotemporal fluctuations and their potential consequences. Temperature and rainfall fluctuate in space and time, according to the findings. In recent times, there has been more unpredictability in temperature and rainfall. In all three districts, *Kiremt* rainfall provides the highest annual rainfall. Except for *Kiremt*, which has a moderate coefficient of variation, annual and seasonal rainfall show substantial inter-annual variability. The percentage of negative deviations varies from 39% (Lay Gayint) to 65% (Simada) over the observation period. The MK test and ITA techniques were applied to the rainfall and temperature data for annual and seasonal time scales. On an annual scale, the results of the MK test showed a significant increasing trend in Lay Gayint and Tach Gayint but a non-significant decreasing trend in Simada. On a seasonal scale, in Simada, *Kiremt* rainfall showed a non-significant decreasing trend, whereas Lay Gayint and Tach Gayint showed non-significant increasing trends. *Belg* rainfall exhibited a non-significant increasing trend in Lay Gayint and Tach Gayint but a non-significant decreasing trend in Simada. The mean seasonal and annual minimum and maximum temperatures exhibited a considerable increasing trend in the study area. The ITA technique results for annual and seasonal rainfall showed positive trends in Lay Gayint and Tach Gayint, while negative trends were detected in Simada. The ITA results for mean annual and seasonal minimum and maximum temperatures showed that the area was warming overall. Climate-sensitive activities, including agriculture and water resource development, are already susceptible to contemporary climate-related threats, as evidenced by annual and seasonal rainfall variability, as well as average annual minimum and maximum temperatures. This suggests the need for climate risk management to be part of local economic development planning in the study area.

ACKNOWLEDGMENTS

We are grateful to Addis Ababa University and Dilla University for their financial assistance to the first author and the Ethiopian National Meteorological Agency for providing climate data gratis.

Disclosure statement

There are no competing interests to declare

Data availability

The data that support the study's findings are available from the Ethiopian National Meteorological Agency, but there are restrictions on their availability because they were used under license for the current study and thus are not publicly available. Data is, however, available from the authors upon reasonable request and with the permission of the Ethiopian National Meteorological Agency.

Author contributions

All authors contributed to the study's conception and design. Material preparation, data collection, and analysis were performed by Aimro Likinaw, Woldeamlak Bewket, and Arragaw Alemayehu. The first draft of the manuscript was written by Aimro Likinaw, and all authors commented on previous versions of the manuscript. All authors read and approved the final manuscript.

REFERENCES

- Abebe G (2017) Long-term climate data description in Ethiopia. *Data Brief* 14:371–392. <https://doi.org/10.1016/j.dib.2017.07.052>
- Abidoye BO, Odusola AF (2015) Climate change and economic growth in Africa: an econometric analysis. *J Afr Econ* 24 (2):277–301
- Ademe D, Ziatchik BF, Tesfaye K, Simane B, Alemayehu G, Adgo E (2020) Climate trends and variability at adaptation scale: Patterns and perceptions in an agricultural region of the Ethiopian Highlands. *Weather Clim Extreme* 29:100263. <https://doi.org/10.1016/j.wace.2020.100263>
- Alemayehu A, Bewket W (2016) Local climate variability and crop production in the central highlands of Ethiopia. *Environ Dev Econ* 19:36–48. <https://doi.org/10.1016/j.envdev.2016.06.002>
- Alemayehu A, Bewket W (2017) Local spatiotemporal variability and trends in rainfall and temperature in the central highlands of Ethiopia. *Geografiska Annaler: Series A, Phys Geogr* 99 (2): 85–101. <https://doi.org/10.1080/04353676.2017.1289460>
- Alemu MM, Bawoke GT (2020) Analysis of spatial variability and temporal trends of rainfall in Amhara Region, Ethiopia. *J Water Clim Chang* 11(4):1505–1520. <https://doi.org/10.2166/wcc.2019.084>
- Amare A, Simane B (2017) Assessment of Household Food Security in the Face of Climate Change and Variability in the Upper Blue-Nile of Ethiopia. *J Agric Sci* 7: pp.285–300. <https://doi.org/10.17265/2161-6264/2017.04.006>
- Asfaw A, Simane B, Hassen A, Bantider A (2018) Variability and time series trend analysis of rainfall and temperature in northcentral Ethiopia: a case study in Woleka sub-basin. *Weather Clim Extreme* 19:29–41. <https://doi.org/10.1016/j.wace.2017.12.002>
- Ayalew D, Tesfaye K, Mamo G, Yitaferu B, Bayu W (2012) Variability of rainfall and its current trend in Amhara region, Ethiopia. *Afr J Agric Res* 7(10):1475–1486. <https://doi.org/10.5897/AJAR11.698>
- Belihu M, Abate B, Tekleab S, Bewket W (2018) Hydro-meteorological trends in the Gidabo catchment of the Rift Valley Lakes Basin of Ethiopia. *Phys Chem Earth* 104:84–101.

- <https://doi.org/10.1016/j.pce.2017.10.002>
- Benti F, Abara M (2019) Trend analyses of temperature and rainfall and their response to global CO₂ emission in Masha, Southern Ethiopia. *Caraka Tani: J Sustain. Agric* 34(1): 67–75. <http://doi.org/10.20961/carakatani.v34i1.28022>
- Berhane A, Hadgu G, Worku W, Abrha B (2020) Trends in extreme temperature and rainfall indices in the semi-arid areas of Western Tigray, Ethiopia. *Environ Syst Res* 9(3): 1–20. <http://doi.org/10.1186/s40068-020-00165-6>
- Bewket W (2009) Rainfall variability and crop production in Ethiopia: case study in the Amhara region. In: Proceedings of the 16th International Conference of Ethiopian Studies. Trondheim: Norwegian University of Science and Technology, Vol. 3: pp. 823–836
- Caloiero T (2018) Application of the innovative trend analysis method for the trend analysis of rainfall anomalies in Southern Italy. *Water Manag* 32(15):4971–4983. <http://doi.org/10.1007/s11269-018-2117-z>
- Chala D, Belay S, Bamlaku A (2020) Analysis of farmers perceived and observed climate variability and change in Didessa sub-basin, Blue Nile River, Ethiopia. *Afr J Agric Res* 15 (2):149–164. <https://doi.org/10.5897/AJAR2019.14054>
- Dinku T, Thomson MC, Cousin R, del Corral J, Ceccato P, Hansen J, Connor SJ (2018) Enhancing National Climate Services (ENACTS) for development in Africa. *Environ Dev Econ* 10 (7): 664–672. <https://doi.org/10.1080/17565529.2017.1405784>
- Diro GT, Tompkins AM, Bi X (2012) Dynamical downscaling of ECMWF Ensemble seasonal forecasts over East Africa with RegCM3. *J Geophys Res* 117:D16103. <https://doi.org/10.1029/2011JD016997>
- Dubache G, Ogwang BA, Ongoma V, Islam T, Md AR (2019) The effect of Indian Ocean on Ethiopian seasonal rainfall. *Meteorol Atmospheric Phys* 131(6):pp.1753–1761. <https://doi.org/10.1007/s00703-019-00667-8>
- Ethiopian Panel on Climate Change/EPCC (2015) First assessment report, Working Group II agriculture and food security, Published by the Ethiopian Academy of Sciences
- Funk C, Nicholson SE, Landsfeld M, Klotter D, Peterson P, Harrison L (2015) The centennial trends greater horn of Africa precipitation dataset. *Sci Data* 2(1):1–17. <https://doi.org/10.1038/sdata.2015.50>
- Gebrechorkos SH, Hülsmann S, Bernhofer C (2019) Changes in temperature and precipitation extremes in Ethiopia, Kenya, and Tanzania. *Int J Climatol* 39(1):pp.18–30. <https://doi.org/10.1002/joc.5777>
- Gebreegziabher Z, Mekonnen A, Bekele RD, Zewdie SA, Kassahun MM (2020) Crop-Livestock inter-linkages and climate change implications for Ethiopia's agriculture: a Ricardian approach. In *Climate Change, Hazards and Adaptation Options* (pp. 615-640). Springer, Cham. http://doi.org/10.1007/978-3-030-37425-9_31
- Gebrehiwot B, Gessesse B, Melgani F (2019) Characterizing the spatiotemporal distribution of meteorological drought as a response to climate variability : The case of Rift Valley Lakes Basin of Ethiopia. *Weather Clim Extreme* 26:100237. <https://doi.org/10.1016/j.wace.2019.100237>
- Getachew B (2017) Impacts of Climate Change on Crop Yields in South Gonder Zone, Ethiopia. *World J Agric Res* 5(2):102–110. <https://doi.org/10.12691/wjar-5-2-6>
- Hamed KH (2009) Enhancing the effectiveness of prewhitening in trend analysis of hydrologic data. *J Hydrol* 368(1-4):143–155. <https://doi.org/10.1016/j.jhydrol.2009.01.040>
- Hamed Khaled H, Ramachandra Rao A (1998) A modified Mann-Kendall trend test for autocorrelated data. *J Hydrol* 204(1-4):182–196. [https://doi.org/10.1016/S0022-1694\(97\)00125-X](https://doi.org/10.1016/S0022-1694(97)00125-X)
- Hundera H, Mpandeli S, Bantider A (2019) Smallholder farmers ' awareness and perceptions

- of climate change in Adama district , central rift valley of Ethiopia. *Weather Clim Extreme* 26:100230. <https://doi.org/10.1016/j.wace.2019.100230>
- Hurni H, Berhe WA, Chadhokar P, Daniel D, Gete Z, Grunder M, Kassaye G (2016) *Soil and Water Conservation in Ethiopia: Guidelines for Development Agents*. Second revised edition. Bern, Switzerland: Centre for Development and Environment (CDE), University of Bern, with Bern Open Publishing (BOP). <https://doi.org/10.7892/boris.80013>
- Kafadar K, Koehler JR, Venables WN, Ripley BD (1999) *Modern Applied Statistics with S-Plus*. *Am Stat* 53(1): 86. <https://doi:10.2307/2685660>
- Kahsay HT, Guta DD, Birhanu BS, Gidey TG (2019) Farmers ' perceptions of climate change trends and adaptation strategies in semiarid highlands of Eastern Tigray, Northern Ethiopia. *Adv Meteorol* 2019:1–13. <https://doi.org/10.1155/2019/3849210>
- Kendall MG (1975) *Rank correlation methods*, 4th edn. Grifn, London
- Mann HB (1945) Nonparametric tests against trend. *Econometrica* 13:245–259. <https://doi.org/10.2307/1907187>
- Mekonen AA, Berlie AB (2020) spatiotemporal variability and trends of rainfall and temperature in the North-eastern Highlands of Ethiopia. *Model Earth Syst Environ* 6:285–300. <https://doi.org/10.1007/s40808-019-00678-9>
- Mesfin D, Simane B, Belay A, Recha JW, Schmiedel U (2020) Assessing the adaptive capacity of households to climate change in the Central Rift Valley of Ethiopia. *Climate* 8(10): p.106. <https://doi.org/10.3390/cli8100106>
- Miheretu BA (2020) Temporal variability and trend analysis of temperature and rainfall in the Northern highlands of Ethiopia. *Phys Geogr* 42(5):434–451. <https://doi.org/10.1080/02723646.2020.1806674>
- Minda TT, van der Molen MK, Struik PC, Combe M, Jiménez PA, Khan MS, de Arellano JVG (2018) The combined effect of elevation and meteorology on potato crop dynamics: a 10-year study in the Gamo Highlands, Ethiopia. *Agric For Meteorol* 262: pp.166–177. <https://doi.org/10.1016/j.agrformet.2018.07.009>
- Nisansala WDS, Abeysingha NS, Islam A, Bandara AMKR (2020) Recent rainfall trend over Sri Lanka. *Int J Climatol* 40(7):3417–3435. <https://doi.org/10.1002/joc.6405>
- Pachauri RK, Allen MR, Barros VR, Broome J, Cramer W, Christ R, van Ypserle JP (2014) *Climate change 2014: synthesis report. Contribution of Working Groups I, II and III to the fifth assessment report of the Intergovernmental Panel on Climate Change* (p. 151). Ipcc.
- Philip S, Kew SF, Jan van Oldenborgh G, Otto F, O'Keefe S, Haustein K, King A, Zegeye A, Eshetu Z, Hailemariam K, Singh R (2018) Attribution analysis of the Ethiopian drought of 2015. *Clim Res* 31(6): pp.2465–2486. <https://doi.org/10.1175/JCLI-D-17-0274.1>
- Rosell S (2011) Regional perspective on rainfall change and variability in the central highlands of Ethiopia. *Appl Geogr* 31(1):329–338. <https://doi.org/10.1016/j.apgeog.2010.07.005>
- Rowell DP, Booth BB, Nicholson SE, Good P (2015) Reconciling past and future rainfall trends over East Africa. *Clim Res* 28(24):pp.9768-9788. <https://doi.org/10.1175/JCLI-D-15-0140.1>
- Sen PK (1968) Estimates of the Regression Coefficient Based on Kendall's Tau. *J Am Stat Assoc* 63(324):1379–1389. <https://doi.org/10.1080/01621459.1968.10480934>
- Şen Z (2012) Innovative Trend Analysis Methodology. *J Hydrol Eng* 17(9):1042–1046. [https://doi.org/10.1061/\(ASCE\)HE.1943-5584.0000556](https://doi.org/10.1061/(ASCE)HE.1943-5584.0000556)
- Wu H, Qian H (2017) Innovative trend analysis of annual and seasonal rainfall and extreme values in Shaanxi, China. *Int J Climatol* 37(5):2582–2592. <https://doi.org/10.1002/joc.4866>